2007 American WJTA Conference and Expo
August 19-21, 2007 • Houston, Texas

Paper

LASER BASED PULSING OF PURE WATER JETS

P. Jäschke, O. Meier, A. Ostendorf
Laser Zentrum Hannover e. V.
Hanover, Germany

Fr.-W. Bach, A. Schenk, C. Filus
University of Hanover
Hanover, Germany

ABSTRACT

Surface treatment as well as cutting of metals, polymers and ceramics using water jet technology, has been established for some time. Compared to conventional techniques such as milling or grinding, the efficiency of the water jet technique is quite low due to low process velocities.
The ablation performance of a water jet can be enhanced by introducing a dynamic component to the jet. This can be achieved by increasing the distance between the nozzle and the work piece, making use of the natural droplet disintegration. However, this results in decreasing energy densities. Furthermore, the accuracy of the treatment becomes worse due to a widening of the water jet.
To address this problem, i.e. achieving a high energy droplet water stream at small standoff distances with a defined impact rate, laser radiation has been used to introduce steam bubbles in close proximity to the nozzle in order to generate a pulsed disruption of the jet.
Investigations on water jet pulsing using CO_2-laser radiation reveal an enhancement of the ablation rate of stainless steel. In order to generate short pulses within the range of 10^{-6} - 10^{-8} seconds, a diode-pumped Q-switched Nd:YAG-laser comes into operation. Due to the lower absorptivity of this laser wavelength within the water jet, dissolvable substrates are added to the water. Using this configuration, pulse frequencies of 40 kHz are realized.

1. INTRODUCTION

Within the water jet technology the continuous pure water jet is typically used for cleaning as well as cutting and ablation processes. It is the ram pressure p_s which is responsible for the impact of the continuous water jet causing a static loading on top of the surface of the work piece. This pressure is proportional to the fluid density ρ_F and to the square of the water jet velocity v.
However, due to internal friction losses within tubes and pipes, the ram pressure is always smaller than the pump pressure p_p, i.e. $p_s < p_p$ [1]. Furthermore, the characteristic of the continuous water jet changes with increasing distance to the orifice. Turbulences within the jet as well as interaction with the environmental media are causing a degradation of the water column into fluid packages and droplets. According to Vijay [2], this partially degraded jet is referred to as naturally pulsed water jet. The dynamic component of the pressure and therefore the amount of droplets and fluid packages increases within the water jet propagation.
It is known that the maximum length of the core of the fluid is 200 times the diameter of the orifice. After this distance the water jet is totally degraded into droplets. The surface of the work piece is then solely treated by droplets causing a dynamic loading. This dynamic pressure p_w is called the water hammer effect and can be calculated with the acoustic velocity in water c_0 to

$$p_w = \rho_F \cdot c_o \cdot v. \tag{1}$$

This pressure is much higher than the ram pressure p_s. A pump pressure of $p_p \approx 70$ MPa causes a dynamic pressure due to droplet impact of approx. $p_w = 570$ MPa [1]. However, with increasing distance to the orifice, the degraded water jet shows a widening which results in a decreased energy density of the water column. A possible way to avoid these disadvantages is to introduce the droplet disintegration directly underneath the orifice due to external impact. According to Vijay, the resulting discontinuous jet is referred to as enforced pulsed water jet [2].

2. GENERATION OF DISCONTINUOUS WATER JETS

A number of different technologies for introducing a pulsation to a continuous pure water jet exist. These technologies can be subdivided into the following categories.

2.1 Mechanical Jet Interruption

The mechanical disruption of a continuous water jet is mostly achieved by a rotating propeller or a hole-plate. The biggest advantage of this method is the possibility of easily setting the pulse length and frequency by varying RPM as well as the propeller or plate geometry. However, there are two major drawbacks. Firstly, the wear on the moving parts due to WJ impingement is very high, and secondly, approximately 75 % of the jet energy is dissipated at the jet breaker. In addition, the achievable pulse rates are limited to a few hundred Hz.

2.2 Variation of Flow Rate by Apertures

A rotating aperture is integrated upstream into the high pressure water flow before the jetting nozzle. This aperture is periodically modulating the water flow and is consequently generating a pulsed jet by the collision of faster and slower water jet particles (Figure 1). However, this technology is limited to a maximum pulse rate of approximately 1000 Hz.

2.3 Ultrasonic Jet Modulation

Vijay [2, 3, 4, 5] developed a setup to generate a pulsed water jet by making use of the piezoelectric and magnetostrictive effect respectively. The transformer oscillation causes a periodic de- and acceleration of the jet (jet velocity modulation). This results in the generation of defined water particles, showing significantly higher erosive potential than continuous water jets [3]. A specific disadvantage of this method is the relatively complex setup due to the high frequency transducer being installed in the high pressure part of the jetting device.

2.4 Self-Resonating Setups

By an adequate arrangement of resonating cavities within the water column before the jetting nozzle, a self-resonating system can be achieved. In [6] Conn et al. describe a number of these setups as shown in Figure 2. Due to the lack of moving parts, this technology is very reliable and cost effective. However, it is not possible to change the dynamic behavior of the water jet except by changing the nozzle design itself.

2.5 Jet Disruption by Electric Discharge

Vijay and Hawrylewicz describe a setup for jet disruption by the discharge of a capacitor [7, 8]. The electric current abruptly evaporates the water within the nozzle or even transforms it into plasma. This method is not only modulating the existing energy supplied by the water supply in form of pressure and water jet velocity respectively, but is even boosting the jetting power by the abrupt increase of volume of the evaporated water portion.

2.6 Cavitating Jets

By placing an obstacle into the upstream water flow before the jetting nozzle, fluid cavitation occurs at adequate flow velocities, i.e. steam bubbles are generated that subsequently disturb the continuous water jet and lead to a disintegration into droplets (Figure 3). The main difference to the methods described before is that this technology is not capable of generating defined pulses but rather a stochastic distribution of droplet sizes and velocities.

3. MOTIVATION

The methods and technologies thus described show specific drawbacks and limitations, above all regarding the maximum allowable fluid working pressure, the maximum pulse rate as well as the wear and tear.

Mostly, these drawbacks are caused by the fact that the generation of the pulses is accomplished upstream of the nozzle within the high pressure part of the jetting system. Consequently, an alternative mechanism for pulsing the water jet itself is studied. One approach to this problem is to make use of a pulsed laser beam to evaporate a small portion of the jet and therefore generating a WJ with defined droplet (segment) sizes and pulse rates.
This technology has two main advantages: Firstly, the pulse generation is decoupled from the jet formation and is therefore separated from the high pressure parts of the system. Subsequently, the latter needs not to be altered and does not bear dynamic loading, so that no problems with wear and tear as well as fatigue damage occur. Secondly, the pulse rate and the droplet sizes (i.e. the length of the water jet segments) can be determined in a very wide range, only limited by the maximum pulse rate of the laser source.

4. EXPERIMENTAL SETUP

The principle setup for the generation of laser pulsed water jets is shown in figure 4. A collimated laser beam of a pulsed laser source is focused into the continuous water jet within a rectangular arrangement. The impact zone of the laser beam is located directly underneath the nozzle in order to ensure an interaction within the core of the water jet. A partial disintegration of the water jet has to be avoided. The working distance between the nozzle and the specimen is also less than 200 times the diameter of the orifice, which is the criterion of being inside the core of the water jet.

4.1 Laser Sources

Within the frame of the investigations two different laser sources came into operation. In order to verify the principle feasibility, a carbon dioxide laser system has been selected. Further experiments have been performed using a solid state laser.
The CO_2-laser used is a high power system emitting a medium output power of $P_L = 2.3$ kW. This laser offers a maximum pulse rate of $f = 500$ Hz with pulse durations of $\tau \geq 1$ ms and a pulse peak power of $P_P = 4.5$ kW.
In order to analyze the pulsation effect at higher frequencies, a diode-pumped Nd:YAG-laser has been used. As a result, the frequency may be increased up to $f = 60$ kHz. This solid state laser is a Q-switched system, which allows the generation of short pulses within the nanosecond-range and higher pulse peak powers compared to CO_2-lasers. The Nd:YAG-laser offers a maximum medium output power of $P_L = 100$ W. However, due to the properties of the Q-switch, pulse peak powers up to $P_P = 200$ kW at pulse durations of $\tau \geq 30$ ns can be realized.

4.2 Absorption Behavior of Water and Modifying Steps

The radiation emitted by a CO_2-laser is located within the long wavelength infrared (LWIR) region at $\lambda = 10.6$ µm. Taking into account the absorption spectrum of water it becomes clear that the radiation of CO_2-lasers will be highly absorbed within the column of a water jet. The absorption coefficient of water at a wavelength of $\lambda = 10.6$ µm is $\alpha_{CO2} = 0.1$ µm^{-1} with a corresponding absorption length of $\Delta x_{CO2} = 0.1$ µm. After a penetration depth of only 0.1 µm, the intensity of the laser beam is decreased to a factor of e^{-1}, thus 64% of the laser power is

absorbed within the first 0.1 µm. According to Lambert-Beer's law of the exponential behavior of radiation within matter [9], the same behavior holds for the following 0.1 µm, etc. Obviously, even for smallest orifice diameters, the radiation of a CO_2-laser will be totally absorbed within the water column. Therefore, no modification of the water is necessary in order to ensure a sufficient energy transfer.

Nd:YAG-lasers are emitting at $\lambda = 1.06$ µm which is located within the near infrared region (NIR). At this wavelength the absorptivity of water is quite small. The absorption coefficient is $\alpha_{YAG} = 10^{-4}$ µm^{-1} which yields to an absorption length of $\Delta x_{YAG} = 10$ mm. Obviously, the radiation of a Nd:YAG-laser will be hardly absorbed within the water column. Even for big orifice diameters, e.g. $d = 300$ µm, only 3% of the laser power will remain within the water.

In order to enhance the absorptivity of water at $\lambda = 1.06$ µm, different additives have been analyzed with respect to dissolubility as well as spectral behavior. Best results have been obtained using a watery suspension based on carbon black nanoparticles. This suspension has been merged with water in different concentrations. Afterwards, spectroscopic investigations have been performed in order to determine the absorption behavior.

The dependency between the carbon black concentration in water and the absorption coefficient is shown in figure 5. The absorption coefficients have been calculated directly from the transmission spectra of each concentration. The measurements have been performed using a fused silica cell with an optical path length of $\Delta l = 100$ µm.

The measurement values reveal a linear increase of the absorption coefficient with the concentration of carbon black in water. This behavior reflects an exponential relation between the optical transmissivity T at a certain wavelength as a function of concentration σ and extinction ε, respectively. According to Lambert-Beer, T is given as

$$T = \frac{I_{\Delta l}}{I_0} = e^{-\varepsilon \cdot \sigma \cdot \Delta l} \quad \text{with} \quad \alpha = \varepsilon \cdot \sigma, \tag{2}$$

where I_0 is the intensity before and $I_{\Delta l}$ the intensity after passing the cell. Obviously, the absorptivity of water can be significantly increased while adding carbon black. Even a concentration of $\sigma = 10^{-3}$ yields to an absorption of $\alpha = 0.002$ µm^{-1}, which is 20 times higher compared to pure water. However, the corresponding absorption length is about $\Delta x = 450$ µm, which is too long with respect to a significant absorption in a water jet originated by an orifice diameter of $d \leq 300$ µm.

Therefore, all experiments with Nd:YAG-laser radiation have been performed using a carbon black concentration of $\sigma = 0.01$, which yields to an absorption coefficient of $\alpha = 0.022$ µm^{-1} and an absorption length of $\Delta x = 45$ µm, respectively.

5. RESULTS

5.1 Generation of Pulsed Water Jets using CO_2-laser

The interaction between a pulsed CO_2-laser beam and a water jet has been documented using a high speed camera. In figure 6, a water jet generated by an orifice diameter of $d = 100$ µm and a fluid working pressure of $p_p = 50$ MPa is given. The disruption within the jet has been induced

by focusing the laser beam into the water column, using a pulse peak power of P_L = 4.5 kW with a pulse duration of τ = 100 ms. The effect of partially evaporated water can be clearly identified.
In order to compare the erosive power of a laser pulsed to a pure water jet, material ablation experiments have been performed. Polished 1.4301 stainless steel specimens were used under a water jet impact angle of 45° in order to reduce back spray of the jet towards the laser optics. The achieved damages on the surface of the work piece have been measured by a stripe projection interferometer and the removed material volume has been computed.
For an orifice diameter of d = 100 µm and a varying fluid working pressure of p_p = 50 to 125 MPa the specimens have been loaded by the pulsed water jet for t = 20 s. Figure 7 shows the ablated volume achieved as a function of the laser frequency. The pulse "on"-time equals the pulse "off"-time during this period. Therefore, the cumulated laser energy applied to the water jet is constant and independent of the frequency.
In spite of high fluctuations within the measurement values of the material removal rates, a clear tendency for an enhancement of the erosive potential of laser pulsed water jets is noticeable. The pulse effect appears at low as well as higher fluid working pressures and increases with increasing frequency. For a working pressure of p_p = 125 MPa, the ablation rate is about 60% higher compared to pure water treatment. For low fluid working pressures, the determined removal rates are in the region of the resolving power of the stripe projection interferometer. Therefore, no conclusion can be drawn with respect to the detailed amount of ablation increase.

5.2 Generation of Pulsed Water Jets using Nd:YAG-laser

In order to investigate the behavior of laser pulsed water jets at higher frequencies as well as shorter pulse lengths, experiments using Nd:YAG-laser radiation have been performed. In contrast to CO_2-lasers, Q-switched Nd:YAG-lasers feature parameter sets consisting of pulse repetition rate f, pulse length τ, pulse peak power P_P and pulse energy E_P, respectively as well as medium output power P_L, whereas these parameters can not be varied independently of each other. The reason for this behavior is the Q-switch, which shares the relatively low medium output power of $P_L \leq 100$ W into short laser pulses ($\tau \geq 30$ ns) generating peak powers up to P_P = 200 kW.
Due to pulse lengths within the range of nanoseconds, it is not possible to use conventional high speed camera technique in order to visualize the interaction between laser beam and water jet. Therefore, the pulse process has been illuminated using a second laser providing a pulse length of τ = 5 ns. This frequency converted Nd:YAG-laser is emitting at a wavelength of λ = 532 nm. Photos have been taken of the sequence with a shutter time much longer than τ but only being exposed during τ. Different stages of the interaction zone are presented in figure 8.
In order to eliminate scattering as well as ambient light, a band pass filter with a center wavelength of λ = 532 nm has been placed in front of the camera. Using this setup it has been possible to generate snapshots of the water jet. Only the center of the interaction zone turned out to be a bright lightened area, caused by the integration over many laser pulses during the shutter time of the camera. However, all other details are representing a time interval of just 5 ns. Image 1 of figure 8 shows an undisturbed water jet generated at a fluid working pressure of p_p = 50 MPa, an orifice diameter of d = 200 µm as well as a concentration of carbon black in water of σ = 0.01. Within images 2 to 5 of figure 8, different stages of the laser pulsing process are depicted. There does not exist a fixed temporal relationship between the images, since the illuminating laser pulses (λ = 532 nm) have not been triggered to the laser pulses interacting with

the water jet (λ = 1064 nm). Nevertheless, the time flow starting with a generation of a compact bubble directly underneath the laser pulsing zone followed by an expansion and a subsequent integration into a constant spray formation can be clearly identified.
Due to the imaging configuration together with the laser- as well as the water-sided parameters it is guaranteed that between the interaction zone of laser and water jet and the beginning of the spray formation, only a single pulse event is captured within the image.
In order to investigate the erosive power of a water jet pulsed by Q-switched Nd:YAG-laser radiation, material ablation experiments have been performed using the aluminum alloy AlMgSi1. Again, the specimens have been loaded under a water jet impact angle of 45°. In this case, kerfs have been generated by linear movement of the specimen relative to the water jet. In order to calculate the removed material volume, kerfs have been measured using a stripe projection interferometer.
Figure 9 shows material removal rates of undisturbed water jet treatment as well as laser pulsed jets at varying fluid working pressure. The water jet originated by an orifice diameter of d = 200 µm has been loaded by laser radiation with a medium output power of P_L = 90 W and a frequency of f = 40 kHz. The laser beam is focused into the water jet in order to ensure absorption at the best possible rate. Using this laser setup, the pulse duration is measured to τ = 210 ns with a pulse energy of E_P = 2.4 mJ.
For $p_p \leq 40$ MPa, both, the measured ablation rates for undisturbed and for laser pulsed water jet treatment are so small that measured values are near the detection limit of the stripe projection interferometer. With rising fluid working pressure the ablation rate of pure water as well as laser pulsation increases, whereas the biggest enhancement of the laser pulsation effect can be found around $p_p \approx 55$ MPa. For higher fluid working pressures the material removal rates of laser pulsed water jet treatment are always higher compared to pure water ablation, however, the ratio of the ablation rates converges against unity, i.e. only a slight effect due to laser pulsing can be determined.
Based on the results achieved within the frame of the working pressure variation experiments, ablation investigations at p_p = 50 MPa and d = 200 µm have been performed. In figure 10, material removal rates of a laser pulsed water jet at a frequency of f = 40 kHz at varying laser output power are presented. In spite of fluctuations within the generated ablation kerfs as well as the complexity of determining the amount of removed material for both, low laser power and pure water jet treatment, a clear tendency for an enhancement of the erosive potential towards higher laser output power is statable.
It is the Q-switch mode of this diode-pumped Nd:YAG-laser which is responsible for the generation of laser pulses. In contrast to CO_2-lasers, higher output powers are not realized by longer pulse durations at constant pulse peak power. Here, the pulse duration decreases with increasing output power. Simultaneously, the pulse energy increases, leading to an enhancement of the pulse peak power towards higher medium output powers. Obviously, E_P and P_P respectively, are the important factors for influencing the properties of the water jet.

6. CONCLUSIONS

Within the frame of the investigations CO_2- as well as Nd:YAG-laser radiation has been used for water jet pulsing experiments. The results are revealing the general feasibility of a laser based water jet pulsing process. The application of high pulse repetition rates of Q-switched Nd:YAG-lasers leads to ablation rates of a multiple of those of undisturbed water jets.
Theoretical considerations lead to the conclusion that the energy transfer from laser radiation to water jet during the absorption process is not sufficient for evaporating the whole illuminated water segment. It can be expected that a partial heating of the water column will result in an expansion of the corresponding water segment and a subsequent rupture of the jet.
Currently, investigations with respect to the significance of pulse frequency, pulse duration as well as pulse peak power are performed. While providing a detailed theoretical model of the interaction process between laser beam and water jet, it is expected that concrete conclusions can be drawn with respect to the properties of the pulsed water jet.

ACKNOWLEDGEMENTS

Part of this work was supported by the “Deutsche Forschungsgemeinschaft” (BU 1395/7-1). The authors would like to thank the DFG for their support.

REFERENCES

[1] Conn, A. F.: On the fluid dynamics of working waterjets – Continuous, pulsed and cavitating. In: Proceedings of the 5th Pacific Rim Int. Conference on Water Jet Technology (1998), page 9/23.

[2] Vijay, M. M. „Pulsed jets: fundamentals and applications“. In: Proceedings in the 5th Pacific Rim International Conference on Water Jet Technology, page 610/627, 1998.

[3] Vijay, M. M.; Foldyna, J. „Ultrasonically modulated pulsed jets“. In: 12th International Conference on Jetting Technology, page 15/36, 1994.

[4] Vijay, M. M.; Debs, E.; Paquette, N.; Puchala, J. R., Bielawski, M. „Removal of coatings with low pressure pulsed water jets“. In: Proceedings of the 9th American Water jet Conference, page 563/580, 1997.

[5] Vijay, M. M.; Foldyna, J. „Ultrasonically modulated pulsed water jets: Effect of the frequency on the performance“. In: Proceedings of the International Conference Geomechanics 96, page 303/308, 1997.

[6] Chahine, G. L.; Conn, A. F.; Johson, Jr.; Frederik, J. S. „Cleaning and cutting with self-resonating pulsed water jets“. In: Proceedings of the 2nd U.S. Water Jet Conference, page 195/207, 1983.

[7] Hawrylewicz, B.M.; Puchala R.J.; and Vijay M.M. Generation of pulsed or cavitation jets by electric discharges in high speed continuous water jets. In: 8th International Symposium on Jet Cutting Technology, page 345/352, 1986.

[8] Vijay, M. M.; Yan, W. and Makomaski, A. Application of ultra-powerful pulsed water jet generated by elektrodischarges. In: 16th International Conference on Water Jetting. BHR Group, 2002.

[9] Alonso, M.; Finn, J.: Physics. Addison-Wesley 1992.

NOMENCLATURE

Symbols

α_{CO2}	[m^{-1}]	absorption coefficient of water at wavelength λ = 10.6 µm
α_{YAG}	[m^{-1}]	absorption coefficient of water at wavelength λ = 1.06 µm
β	[-]	orifice efficiency
d	[m]	orifice diameter
ε	[m^{-1}]	extinction coefficient
Δl	[m]	optical path length within spectroscopic measurements
Δx_{CO2}	[m]	absorption length for wavelength λ = 10.6 µm in water
Δx_{YAG}	[m]	absorption length for wavelength λ = 1.06 µm in water
E_P	[J]	pulse energy
f	[Hz]	pulse repetition rate, frequency
I_0	[W/m²]	spectroscopy: light intensity before passing the cell
$I_{\Delta l}$	[W/m²]	spectroscopy: light intensity after passing the cell
λ	[m]	laser wavelength
P_L	[W]	medium output power
P_P	[W]	pulse peak power
p_p	[Pa]	pump pressure
p_s	[Pa]	ram pressure
p_w	[Pa]	dynamic pressure
σ	[-]	volume concentration
t	[s]	time
τ	[s]	pulse duration, pulse length
T	[-]	transmissivity
v	[m/s]	water jet velocity

Constants

c_0	acoustic velocity in water	1480	m/s
ρ_F	density of water	1000	kg/m³

Abbreviations

CO_2-laser	gas laser; type: carbon dioxide
LWIR	long wavelength infrared (8 to 15 µm)
Nd:YAG-laser	solid state laser; type: Neodym Yttrium Aluminum Garnet
NIR	near infrared (0.7 to 1.4 µm)
Q-switch	Acousto-optic modulator inside a laser resonator

GRAPHICS

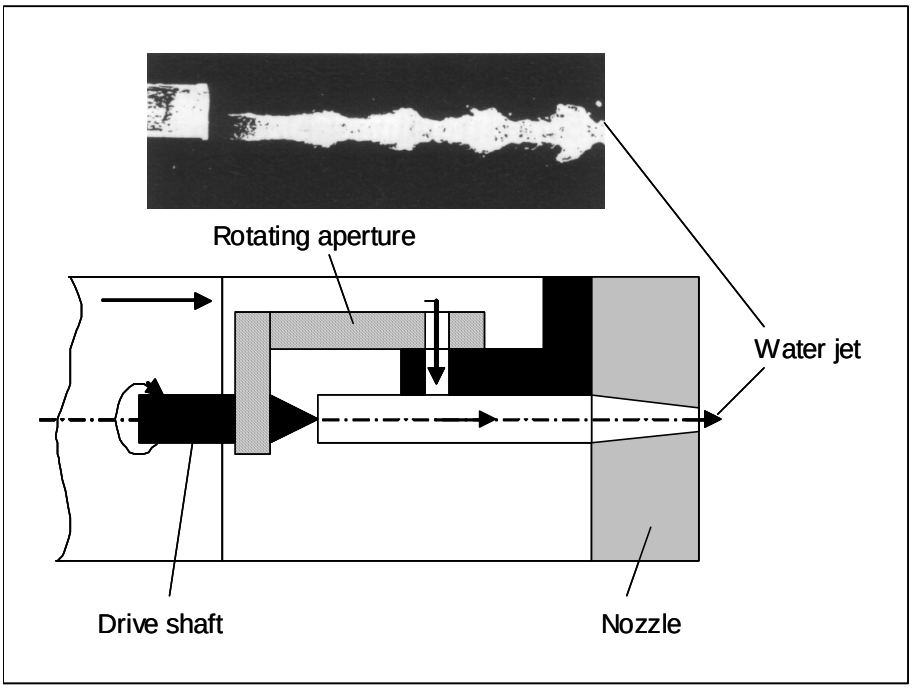

Figure 1. Percussive jetting according to Nebeker.

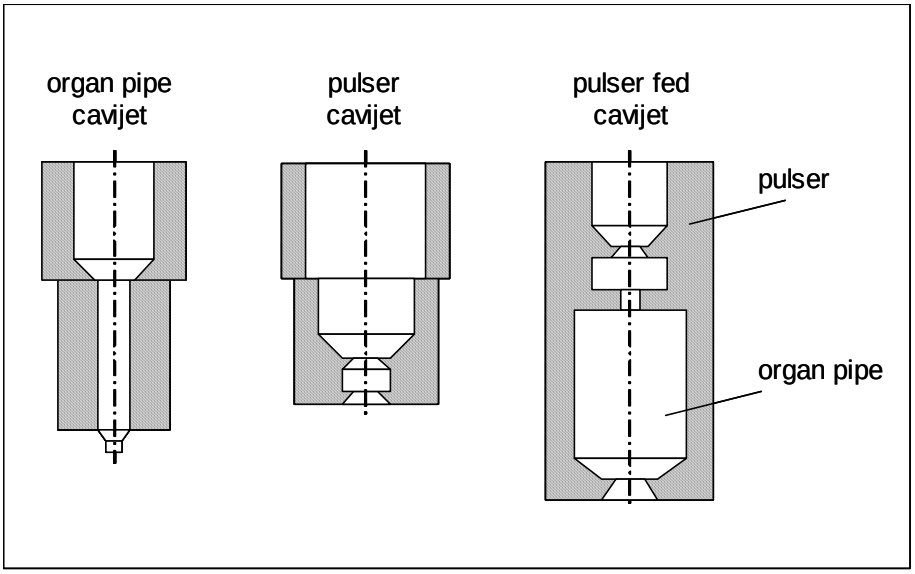

Figure 2. Nozzle concepts for self-resonating systems [6].

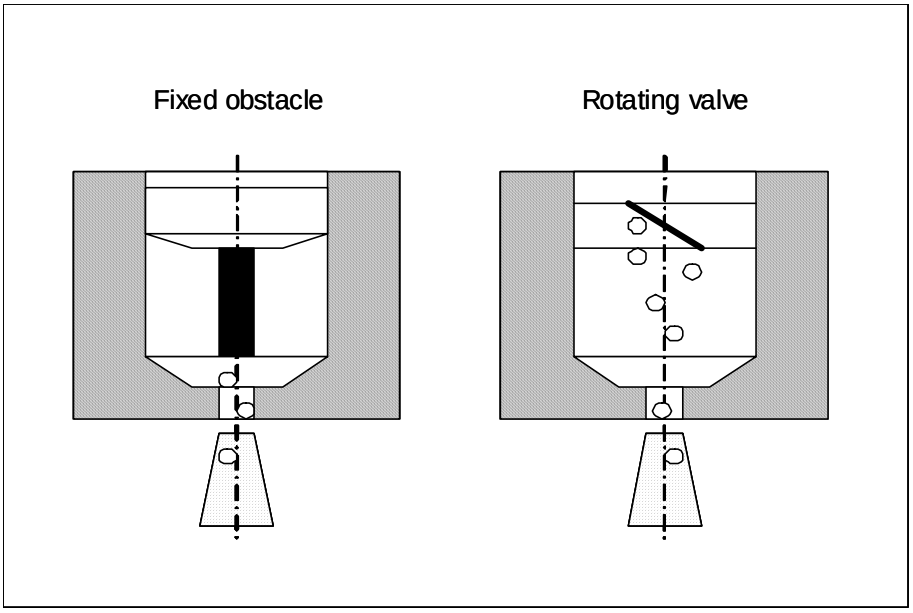

Figure 3. Cavitating jets.

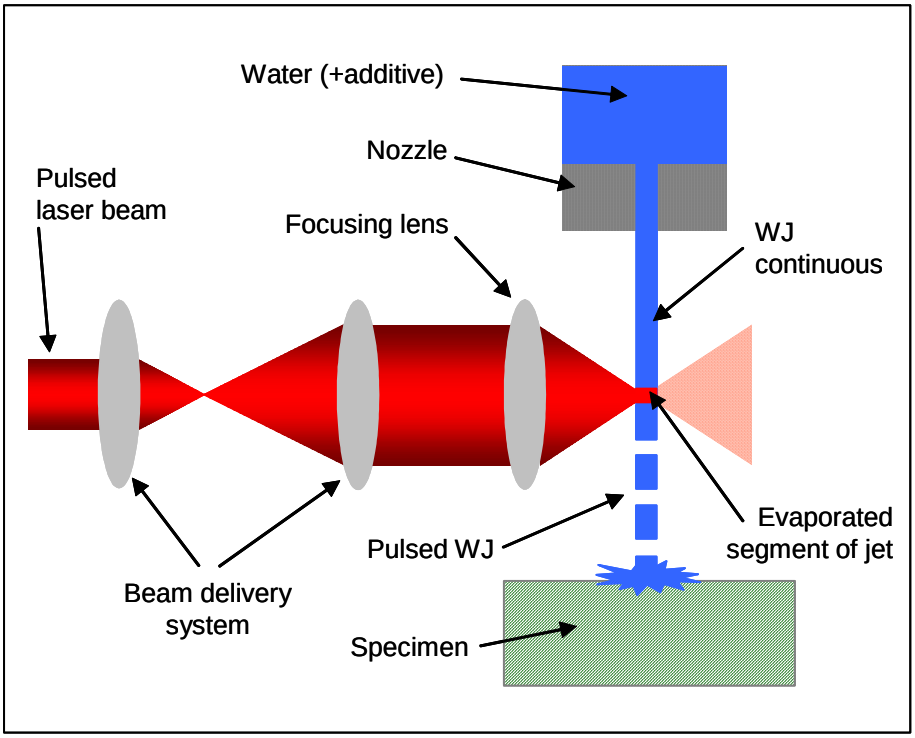

Figure 4. Principle setup for generating laser pulsed water jets.

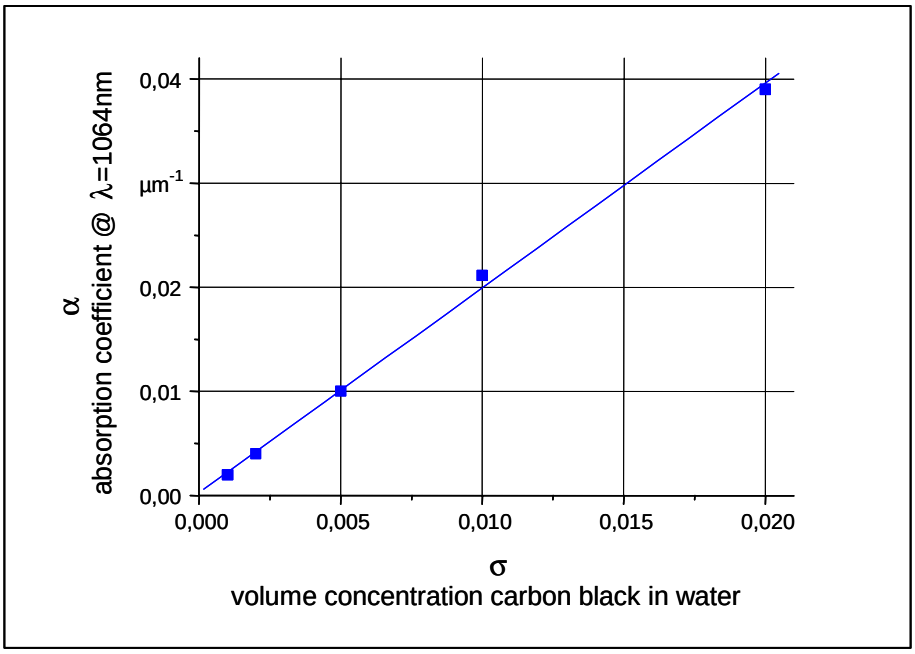

Figure 5. Dependency of absorption coefficient on carbon black concentration.

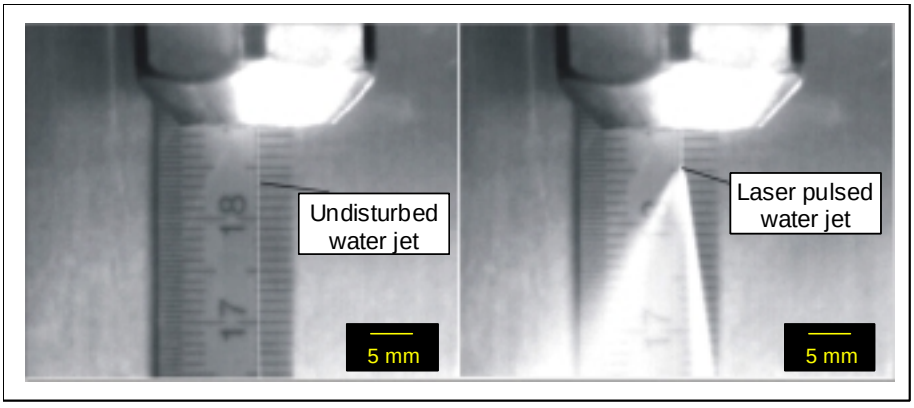

Figure 6. Water jet, undisturbed and pulsed by CO_2-laser radiation.

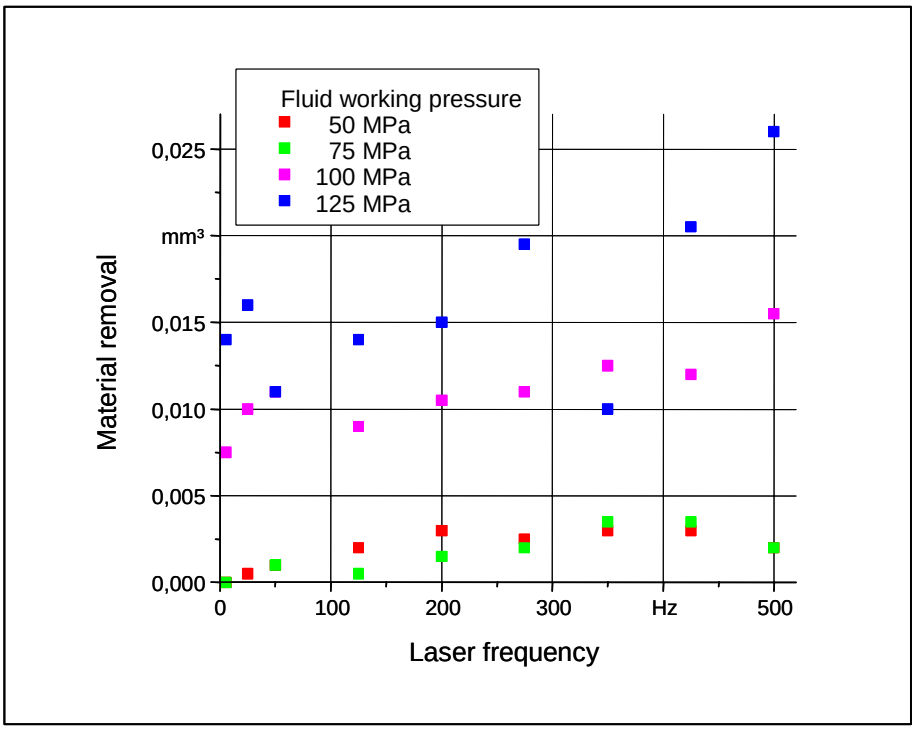

Figure 7. Material removal for different working pressures at varying pulse frequency and constant CO_2-laser output power.

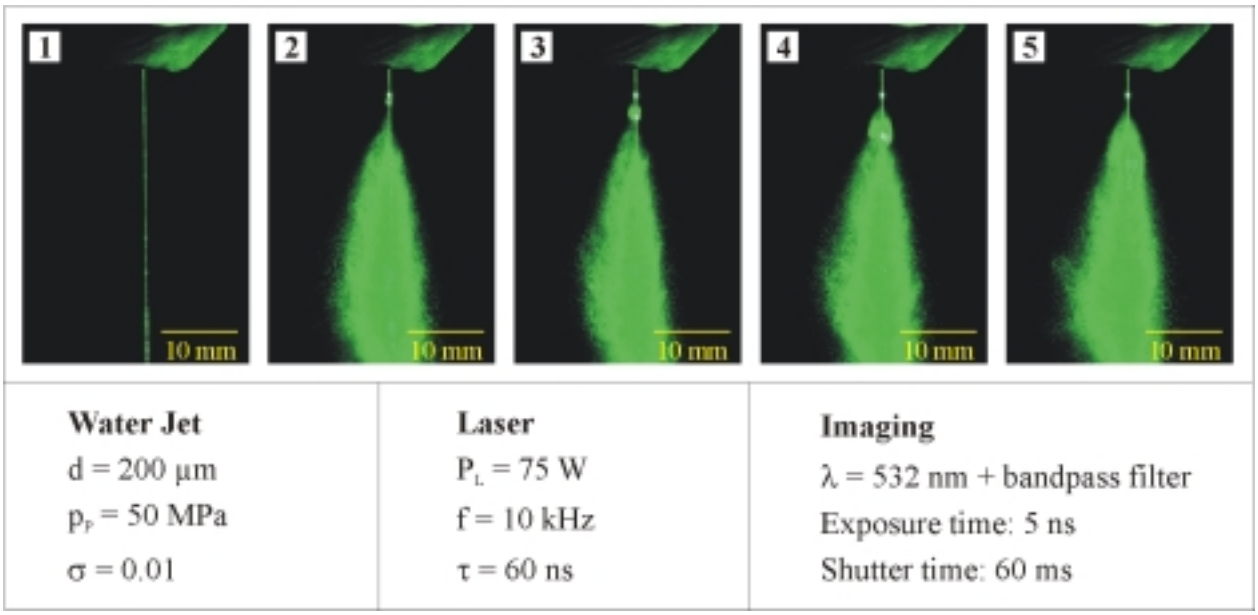

Figure 8. Water jet, undisturbed (1) and pulsed by Q-switched Nd:YAG-laser radiation (2-5).

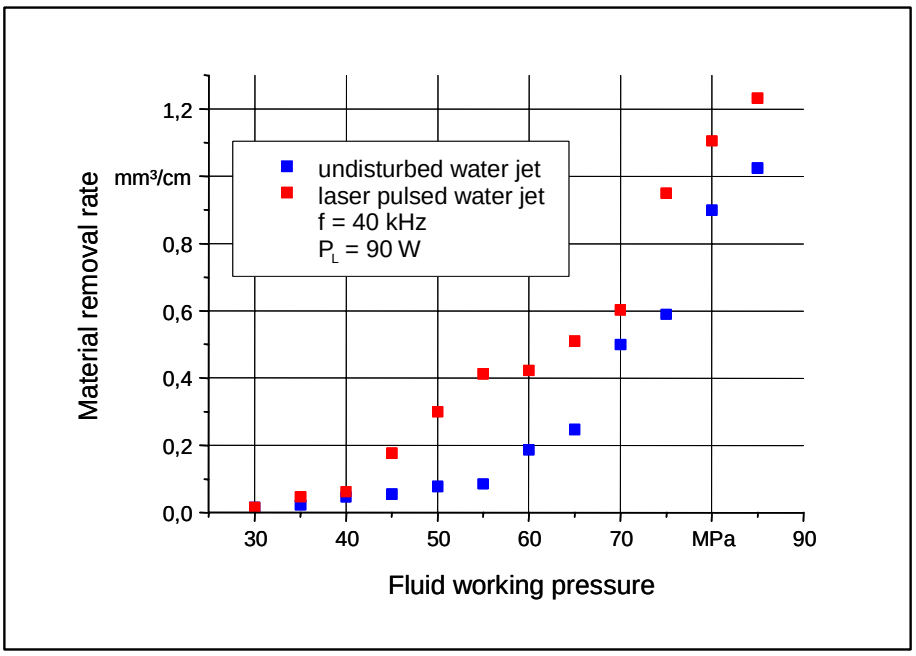

Figure 9. Comparison of ablation rates of undisturbed and laser pulsed water jet treatment as a function of working pressure.

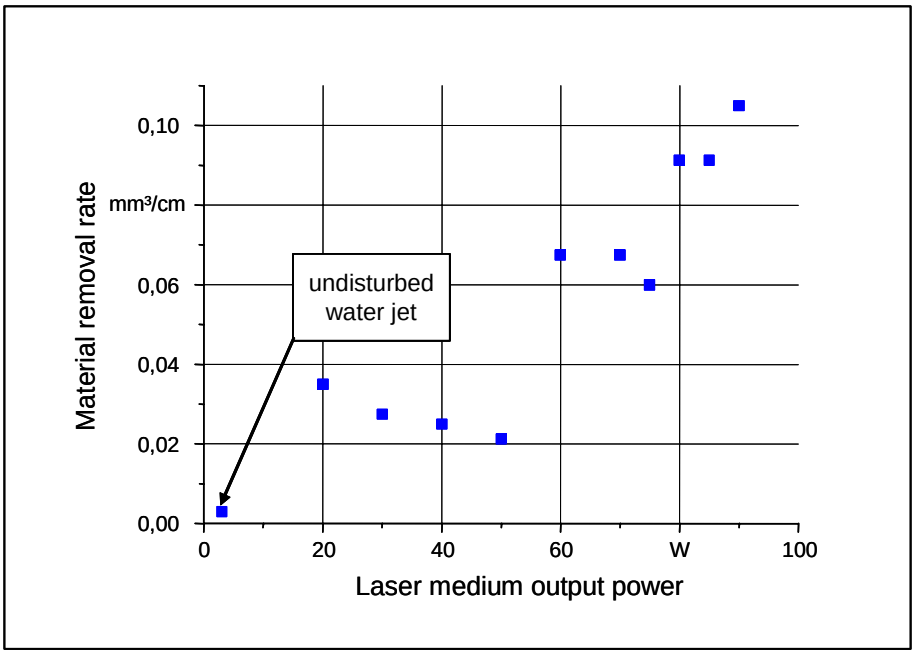

Figure 10. Ablation rates for laser pulsed water jet treatment as a function of laser output power (f = 40 kHz).